PROTEINS: Structure, Function, and Genetics 2:167–176 (1987)

Structure of an Insect Virus at 3.0 Å Resolution

M.V. Hosur,[1] T. Schmidt,[1] R.C. Tucker,[1] J.E. Johnson,[1] T.M. Gallagher,[2] B.H. Selling,[2] and R.R. Rueckert[2]
[1]*Department of Biological Sciences, Purdue University, West Lafayette, Indiana 47907;* [2]*Biophysics Laboratory, Graduate School and Department of Agriculture, College of Agriculture and Life Sciences, University of Wisconsin, Madison, Wisconsin 53706*

ABSTRACT **We report the first atomic resolution structure of an insect virus determined by single crystal X-ray diffraction. Black beetle virus has a bipartite RNA genome encapsulated in a single particle. The capsid contains 180 protomers arranged on a $T = 3$ surface lattice. The quaternary organization of the protomers is similar to that observed in the $T = 3$ plant virus structures. The protomers consist of a basic, crystallographically disordered amino terminus (64 residues), a β-barrel as seen in other animal and plant virus subunits, an outer protrusion composed predominantly of β-sheet and formed by three large insertions between strands of the barrel, and a carboxy terminal domain composed of two distorted helices lying inside the shell. The outer surfaces of quasi-threefold related protomers form trigonal pyramidyl protrusions. A cleavage site, located 44 residues from the carboxy terminus, lies within the central cavity of the protein shell.**

The structural motif observed in BBV (a shell composed of 180 eight-stranded antiparallel β-barrels) is common to all nonsatellite spherical viruses whose structures have so far been solved. This highly conserved shell architecture suggests a common origin for the coat protein of spherical viruses, while the primitive genome structure of BBV suggests that this insect virus represents an early stage in the evolution of spherical viruses from cellular genes.

Key words: icosahedral, insect, virus, structure, evolution, nodavirus

INTRODUCTION

Black beetle virus (BBV) is a ribovirus first isolated from the larvae of the beetle *Heteronychus arator*. Injections of purified virus cause fatal paralysis in a variety of lepidoptera.[1] BBV grows vigorously in cultured *Drosophila* cells, producing yields as high as one-fifth of the total cell protein within 3 days.[2] BBV is a member of the family Nodaviridae,[3,4] which are the only known nonenveloped animal viruses that display a $T = 3$ surface lattice and contain a bipartite genome, although both of these characteristics are common among isometric plant viruses.[5] Table I lists physical properties of the BBV particle and properties of the RNA and protein molecules derived from the sequences of the bipartite genome.[6,7] The two RNA molecules are encapsulated in the same particle.[8,9]

RNA1 contains the replicase gene and encodes two proteins, A and B[10] whose replicative functions have yet to be precisely defined. RNA2 encodes the coat protein α,[7] which is found in virions together with two other proteins, β and γ (Fig. 1); β and γ are generated by the proteolytic cleavage of protein α, but the role of this cleavage in acquisition of infectivity and the morphogenetic step at which it occurs are still unclear.

We report here the structure of BBV, the first high-resolution analysis of an insect virus by single crystal X-ray diffraction, and the identification of the subunit cleavage site established from sequence analysis of the β and γ peptides.

MATERIALS AND METHODS

Crystallography

Crystals of BBV were grown as reported,[13] were cubic, and belonged to space group $P4_232$, $a = 362$ Å with two particles per cell. The particles were positioned at tetrahedral symmetry sites in the lattice, thus only the fivefold axes of the icosahedral particles did not coincide with the lattice symmetry axes. Heavy-atom derivatives were prepared by soaking native crystals in solutions of dipotasium tetrachloroplatinate or fluorescein mercury acetate. Scaling statistics for the native and derivative data sets as well as details of the data collection are given in Table II. The heavy atom positions in the mercury derivative (A,B,C; Table III) were determined using the Patterson noncrystallographic vector search procedure[16] as were sites D, E, and H in the platinum derivative. The sites found in the search function were refined, and phases were computed. Difference Fourier maps calculated using these phases revealed two additional sites (F and G) in the platinum derivative but no additional sites in the mercury derivative. Double isomorphous replacement derivative phases were calculated to 5.0 Å resolution, and a native electron density map was computed. The map

Received May 18, 1987; accepted July 15, 1987.

Address reprint requests to J.E. Johnson, Department of Biological Sciences, Purdue University, West Lafayette, IN 47907.

M. V. Hosur's present address is Bhabha Atomic Research Centre, Neutron Physics Division, Trombay, Bombay 40085, India.

was averaged using the noncrystallographic fivefold symmetry,[17] which revealed a distinct envelope of density in the region expected for the protein shell. An envelope was defined using the electron density distribution observed in the averaged map and the interparticle contact distances along the body diagonal of the crystal cell. Electron density outside of this envelope was set to zero, and a Fourier transform of the averaged, solvent leveled map was computed. The calculated phases were then combined with the observed amplitudes, and weights were calculated as described.[18] This procedure was continued at 5.0 Å resolution until the average phase change in the calculated structure factors was less than 5° when compared with the previous cycle. Phases were then extended to 3.0 Å resolution in 27 increments.[18] The overall R factor and correlation coefficient, as defined in Rossmann et al.[18] were 20.0% and 0.84, respectively. The details of the crystallographic analysis will be reported elsewhere.

Location of Cleavage Site in Protein Alpha

Purified [^{35}S]-methionine-labeled virions (0.55 mg; 3.9×10^6 dpm in 0.25 ml 0.1% sodium dodecyl sulfate [SDS], 0.01 M-NH_4HCO_3, pH 8.1) were heated 2 min in a boiling water bath and the slightly turbid suspension, RNA and all, was analyzed in a gas phase protein sequencer (Applied Biosystems Model 370A) equipped with a Model 120A PTH amino acid analyzer. Only one major sequence, A-S-M-W-E-R-V-K-S-I-I-K, was found. The yield of this peptide was only 32% of the expected value, perhaps because of incomplete dissociation of the virus, which is extraordinarily stable. Nonetheless, the sequence matched that of amino acid residues 364–375 in the coat precursor, α, deduced from the sequence of RNA2.[7] We conclude that the amino termini of the α and β chains were blocked; and that the chain is identical with the carboxyterminal 44 amino acid residues of the α chain.

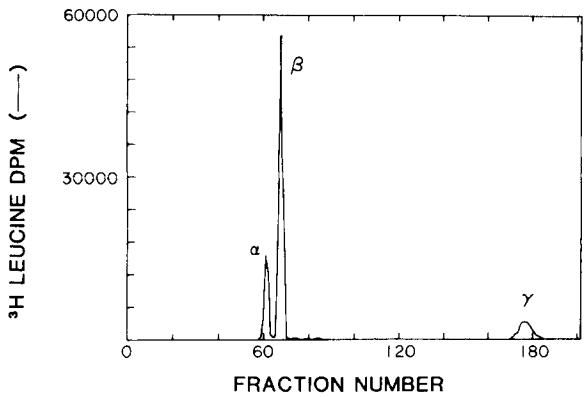

Fig. 1. Profile illustrating the distribution of radioactivity in coat proteins of [^{3}H]-leucine-labeled BBV (160,000 dpm) after electrophoretic separation on SDS polyacrylamide gel.[11] The cylindrical gel was crushed, fractionated, and counted as described.[12] Migration was to the right. The distribution of radioactivity was: α, 20%; β, 66.8%; and γ, 13.2%.

Molar Proportion of Mature and Immature Subunits in the Virion

Purified tritiated leucine labeled virions were analyzed for the ratio of α to β and γ. Given the amino acid sequence of the α chain[7] and the location of its cleavage site between Asn 363 and Ala 364, the leucine content of each chain is expected to be α, 24; β, 20; γ, 4. From the distribution of radioactivity (Fig. 1) the ratio of β to γ chains was calculated to be 1.01. Thus, it appears that no γ chains are lost from virions when the "immature protomer" (α chain) is cleaved to form the "mature" protomer (β + γ chain). The α chain content varied from 10% to 25% for different virus preparations.

RESULTS AND DISCUSSION

Electron Density Map

The 3.0-Å electron density map of the BBV particle revealed a well-ordered capsid protein structure. The

TABLE I. Properties of Black Beetle Virus

Properties of the particle					
Spherically averaged diameter					312 Å (solution X-ray scattering)
Percent RNA (weight)					16
Molecular weight					9.4×10^6 daltons
Sedimentation coefficient					137 S
Buoyant density					1.33 g/cc
Properties of the capsid protein					
	43 kD		38 kD	5 kD	
	α(407AA)	→	β(363AA)	+ γ(44AA)	
The 180 promoters in the $T = 3$ capsid are composed of approximately 10–25% α, and the rest are β + γ.					
Properties of the RNA molecules[6,7]					
	M.W. (daltons)	No. of bases	No. of proteins	5′OH	3′OH
RNA1	1.0×10^6	3,105	2	Capped	Probably a protein
RNA2	0.5×10^6	1,399	2	Capped	Probably a protein

TABLE II. Data Collection and Processing*

	Native†	Fluorescein mercury acetate‡	Platinum chloride**
Resolution	50–3.0 Å	50–5 Å	50–5 Å
No. measured	394,197	37,573	32,374
No. unique¶	110,726	23,385	19,958
Percent of data	72	71	60
Agreement factor(%)§	13	12	11

*Diffraction data were processed and scaled using the oscillation photograph processing programs developed by M.G. Rossmann and colleagues.[14,15]

†Native data were collected at the Laboratoire pour l'Utilization du Rayonnement Electromagnetique (LURE), Orsay, France. A total of *68* film packs were collected using a 0.3° oscillation angle with 30-minute exposure times. Two photographs were taken with each crystal. Five films were not used in the data set because of poor scaling. The crystals were mounted with the 1$\bar{1}$0 direction coincident with the spindle axis. The zero spindle angle was defined as c*, perpendicular to the X-ray beam.

‡The derivative was prepared by soaking BBV crystals in a solution composed of 3 mM fluorescein mercury acetate, 30 mM sodium phosphate pH 8.5, and 0.5 M Na_2 SO_4 for 10 hours. The derivative data were collected at the Cornell High Energy Synchrotron Source (CHESS), Cornell University, Ithaca, New York. A total of 18 film packs were collected using a 1° oscillation angle and an exposure time of 2 minutes. The crystals were small and extremely radiation sensitive; thus only one photograph was obtained per crystal.

**The derivative was prepared by soaking BBV crystals in 4 mM K_2PtCl_4, 30 mM potassium phosphate pH 7.0, and 1 M Na_2SO_4 for 12 hours. The derivative data were collected using a rotating anode X-ray source (Elliot GX20). A total of 18 1° photographs were recorded using an exposure time of 12 hours per photograph.

¶Only data for which $\frac{I}{\sigma(I)} \geq 2.0$ were used for the data set.

§$R = \frac{\Sigma_h |I_h - \bar{I}_h|}{\Sigma_h I_h}$.

TABLE III. Refined Heavy Atom Parameters*

Derivative	Site	Relative occupancy	No. of sites per virion	Fractional cell coordinates X	Y	Z	Orthogonal coordinates† P	Q	R
Fluorescein mercuric acetate	A	69.7	60	0.03529	0.13234	0.34416	12.8	47.9	124.6
	B	74.5	60	−0.06094	0.08120	0.34438	−22.1	29.4	124.7
	C	60.9	60	0.02423	0.02856	0.33655	8.8	10.3	121.8
	D Fivefold axis	54.0	12	0.0	0.23529	0.38067	0.0	85.2	137.8
	E Threefold axis	22.4	20	0.14388	0.00	0.37678	52.1	0.0	136.4
Dipotassium chloro-platinate	F Fivefold axis	8.8	12	0.00	0.21205	0.34307	0.00	76.8	124.2
	G Threefold axis	48.9	20	0.13402	0.00	0.35097	48.5	0.0	127.1
	H '5-3' edge	83.5 0	30	0.06697	0.11792	0.37983	24.2	42.7	137.5

*The refinement was based on 14,802 reflections for which native and both derivative amplitudes were measured. The maximum resolution was 5.0 Å, and the overall DIR figure of merit to this resolution was 0.537.

†Coordinates for heavy atoms in one icosahedral asymmetric unit are given. P, Q, R correspond to the position in Å relative to the particle center. The P, Q, and R directions are coincident respectively with the X, Y, Z crystallographic axons.

RNA core is not visible in the electron density because it lacks the symmetry necessary for detection by the crystallographic method. The shell is composed of 60 triangular units arranged with icosahedral symmetry. A portion of the electron density in one of these units is shown in Figure 2. Each triangular unit consists of three identical polypeptide chains (Fig. 3B) arranged with approximate threefold sym-

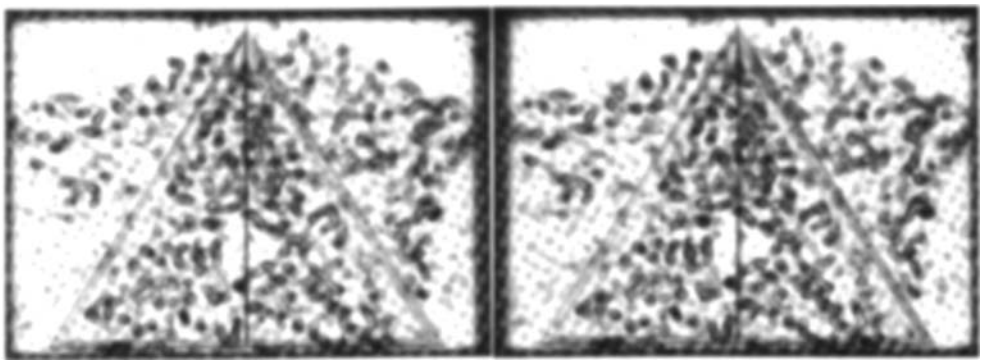

Fig. 2. A stereoscopic view of a slab of electron density between 133 and 143 Å from the particle center, cut perpendicular to an icosahedral twofold axis. The triangular wedge outlines one icosahedral asymmetric unit described in more detail in Figure 3b. The quality of the map is illustrated by the connectivity of the density, the quasi-equivalence of the density about the centroid of the triangle, and the contrast between solvent and protein, particularly between the fivefold and threefold axes where the subunits in contact are splayed out and solvent leveling was not applied. The clear regions at the top of the figure were explicitly solvent leveled.

metry to form the *icosahedral asymmetric unit* characteristic of a $T = 3$ surface lattice.[19] The quasi-equivalent positions of the three chains that make up the asymmetric unit are distinguished by color and letter codes: blue (A), red (B), and green (C) (Fig. 3b). Each of the three polypeptide chains was readily traced in a map at 3.7 Å resolution. A model derived from the primary structure, including side chains, was successfully fitted to the 3 Å electron density map using the program FRODO[20] and an Evans and Sutherland PS300 graphics system. The orientation of a folded "green" subunit (protomer) is illustrated in more detail in Figure 3A. The term protomer refers to protein α *or* its cleavage product ($\beta + \gamma$).

Figure 3B illustrates the organization of a single icosahedral asymmetric unit. The three protomers form a prominent terraced pyramid (center of Fig. 3B), which rises to a peak. This is shown in Figure 3c, which illustrates a cross-section of the shell from the inside of the particle (bottom) to the outside (top). The arrangement of the 60 asymmetric units in the intact particle is shown in Figure 3D. The electron density can be divided into three layers; a 25-Å-thick central layer lying 120 to 145 Å from the center of the particle, a lower layer extending down to 100 Å, and an upper layer reaching out as far as 166 Å. The central layer carries the bonding contacts between asymmetric units and forms the continuous part of the closed shell (contiguous shell). The bottom layer on the inner surface of the shell is composed of six helical segments that extend into the central cavity.

Protomer Structure

Nucleotide sequencing predicts that the protomer consists of 407 amino acids[7]. Segments of the chain containing residues 1–64 and residues 345–407 were invisible in the electron density map, which indicated that these portions of the chain are disordered. The visible termini, ala 65 and Leu 344, lie internally and only 6 Å apart. The invisible portion of the chain, from residues 1 to 64, probably adapts to the various conformations of the RNA; it contains 17 basic amino acids capable of neutralizing the negatively charged phosphate residues of the nucleic acid. This interpretation is consistent with previous structural and chemical studies of plant viruses.[21–13] The visible carboxyterminus of the BBV protomer, unlike that of other spherical viruses, lies internally. This difference may be related to the presence of a cleavage site within the invisible carboxy-terminal end of the protomer, a feature unique to nodaviruses.

The contiguous shell density and the surface pyramid are made up of residues 92–310 (Fig. 3A). The dominant folding feature is an eight-stranded antiparallel β-barrel (organized in the β-roll topology[25]), which is very similar to the wedge-shaped subunit core seen in other plant and animal virus structures.[18,21,22,26,27] The connections between strands at the narrow end of the wedge are tight turns containing no more than five residues. At the broad end of

Fig. 3. Organization of black beetle virus established from the 3.0-Å electron density map. The central portion of the figure, labeled with small letters, provides expository information for the outer portion of the figure labeled with large letters. Each of the identical capsid subunits (**A**) consists of an eight-stranded antiparallel β-barrel (dark green) with three major loops (light green) inserted between strands of the barrel. The strands of the β-barrel are labeled according to the standard convention established for other viral coat proteins.[22] Although the chain consists of 407 amino acids, only those from residue 65 to 344 were visible in the electron density map. The invisibility of residues 1–64 and of 345–407, containing the cleavage site, indicates that these portions of the chain are disordered. The subunits are organized into tightly associated trimeric clusters that make up the icosahedral asymmetric unit (**b,B**). The space filling representations were generated by placing a sphere of 3 Å radius at each Cα position. Each color represents one of the three quasi-equivalent positions. The three major loops of each subunit are terraced to form a prominent pyramid on the virion surface. This is most evident in a side view of the trimeric cluster (**c,C**). The three underlying appendages intruding into the central cavity of the shell are distorted helices formed by residues 320–344 of each subunit. The intact virion (**d,D**) consists of 60 trimeric clusters (b,B) arranged with icosahedral symmetry encapsulating both parts of the bipartite RNA genome. The green and red subunits are clustered about threefold icosahedral symmetry axes in the assembled particle, and the blue subunits are adjacent to fivefold axes. (d,D).

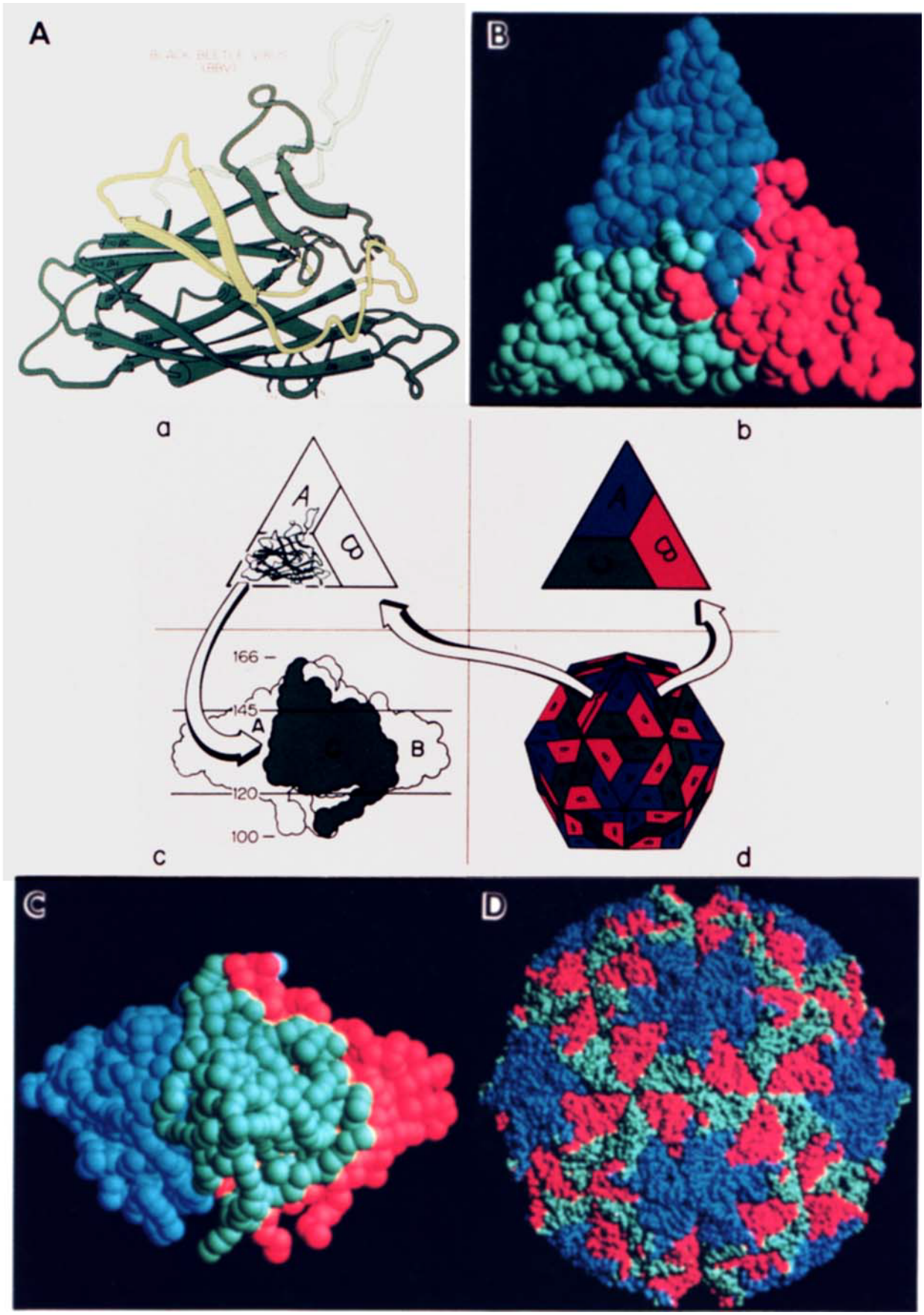

Fig. 3.

the wedge there are large insertions between βC and βD (50 residues; Fig. 3A), between βE and βF (34 residues), and between βG and βH (45 residues). All of these insertions extend toward the outer surface of the virion. Together they form one-third of a prominent pyramidal terrace on the surface of the virus (see below). The βC-βD insertion and the βG-βH insertion contain four β-strands in such close association with the core as to extend the F, E, H, C side of the β-barrel into an eight-stranded sheet. The insertion between βE and βF is particularly remarkable in that it forms a two-stranded β structure extending from the lower portion of the barrel to the apex of the terraced pyramid.

At the end of βI the chain makes an excursion below the contiguous shell and forms two helices, which together form the prominent appendages seen in Figure 3C. The first helix is an α, while the second is more extended. An unusual feature of this appendage is that it is solidly tethered to the barrel through a hydrophobic interaction between Phe 240 in βG and Phe 332 in the first helix. No other spherical virus shows such a prominent internal feature.

Quaternary Structure

The contiguous shell of BBV is formed by a region of the protein that lies 120 to 145 Å from the center of the particle (Fig. 3c). This portion of the shell has the shape of a rhombic triicontahedron[22] (Fig. 3d). Each of the asymmetric units (Figs. 3b,B) abuts three neighboring asymmetric units: one at its base and two at its sides. This should be evident by inspection of Figure 3d. The shape of the shell is due in part to differences in the angle at which the asymmetric units join at the base (icosahedral twofold joint) and at the two sides (quasi-twofold joints). The symmetry relationships between neighboring asymmetric units are illustrated in Figures 4A and 4B. Asymmetric units joined at the icosahedral twofold joint (Fig. 4c) lie in the same plane (dihedral angle 180°) forming a flat diamond-shaped surface. Asymmetric units at the quasi-twofold joint, by contrast, form a 136° dihedral angle (Fig. 4d). It should be apparent from inspection of the polypeptide backbone diagram shown in Figure 4A that the contacts between subunit A (blue) and subunit B5 (red) (refer to subunit nomenclature in Fig. 4B) are similar to contacts between green subunits C and C2. The icosahedral twofold joint in Figure 4c or C is prevented from bending by an extended protein chain inserted into a hydrophobic groove between the C and C2 subunits (represented as the sawtooth contact in Fig. 4B). This inserted chain is not found between the A and B5 subunits at the quasi-twofold joints (smooth contact in Fig. 4B). In the latter case the hydrophobic surfaces of the groove interact directly with each other (Fig. 4d,D).

The architecture of BBV strongly resembles that of two $T = 3$ plant viruses, tomato bushy stunt virus (TBSV) and southern bean mosaic virus (SBMV).[21,22] Moreover, the presence of a protein segment, often called an "arm," in the icosahedral but not in the quasi-twofold joints, is a feature common to all three viruses, but the details in BBV are different. In the case of the plant viruses, the arm is contributed by the C subunits and constitutes an additional strand (βA), which is connected directly to βB in the β-barrel; this strand is invisible in the plant virus A and B subunits. In BBV, however, the arm in the occupied twofold groove is disordered at both termini and is *not* connected to the βB strand of the C subunit. The chemical sequence of the portion of the subunit that corresponds to this arm is not yet clear. Of the unassigned amino acid residues, the likeliest candidate is part of the polypeptide between residues 376 and 407, i.e., residues 13–44 of the γ chain. This region, unlike other unassigned protein, is predominantly hydrophobic and contains few charged side chains. A second difference between the plant and insect viruses is that the visible amino termini in the A, B, and C subunits, corresponding to residues 65–92 prior to βB, are quasi-equivalent in BBV; the plant viruses show no quasi-equivalence prior to βB.

Prominent clefts in the surface of the virion are apparent in Figure 3D (top and bottom of the particle). These clefts are formed by the sides of the pyramids rising from the center of the asymmetric units at planar icosahedral twofold joints (Fig. 4C). At the bent quasi-twofold joints these pyramids are tilted away from each other and present much more gradual slopes (Fig. 4D).

Virus Structure and Evolution

Atomic structures have now been determined for the protein shells of a number of spherical viruses infecting plants, mammals, and insects (Table IV). With the single exception of satellite tobacco necrosis

Fig. 4. Differences in bonding interactions at the icosahedral and quasi-symmetry axes determine the shape of the shell. This figure is arranged as in Figure 3. **A** and **B** show the asymmetric unit and its symmetry relationships to adjacent subunits. Subunits are represented as colorcoded α-carbon backbones in A and as ABC in bB; this follows the standard convention used in describing other $T = 3$ viruses.[21,22] Lines in A delineate the inner and outer limits of the contiguous shell and connect the threefold and fivefold vertices to the particle center. Icosahedral symmetry axes are indicated in B by white symbols: pentamer (fivefold axis); triangle (threefold), and ellipse (twofold). The joints between subunits related by icosahedral or quasi-twofold symmetry axes are shown in red; joints between subunits related by icosahedral fivefold or quasi-sixfold axes in yelllow; and joints between subunits related by quasi-threefold axes in green. Quasiequivalence theory predicts that all contacts of the same color are similar but need not be identical. **c,C** and **d,D** illustrate the difference in dimeric bonding interactions at twofold and quasi-twofold joints. c,C shows the joint at the icosahedral twofold axes (sawtooth red joint, B) while d,D show the joint at the quasi-twofold axes (smooth red line, B). The difference is due to a segment of protein that prevents the subunits from pivoting about the hinge at the icosahedral twofold joint. This segment is not present under the hinge at the quasi-twofold joint. If all of the contacts were flat, as in C, the protein assembly would form a sheet. Thus the bent contact at the quasi-twofold joint provides the curvature required to form a spherical shell.

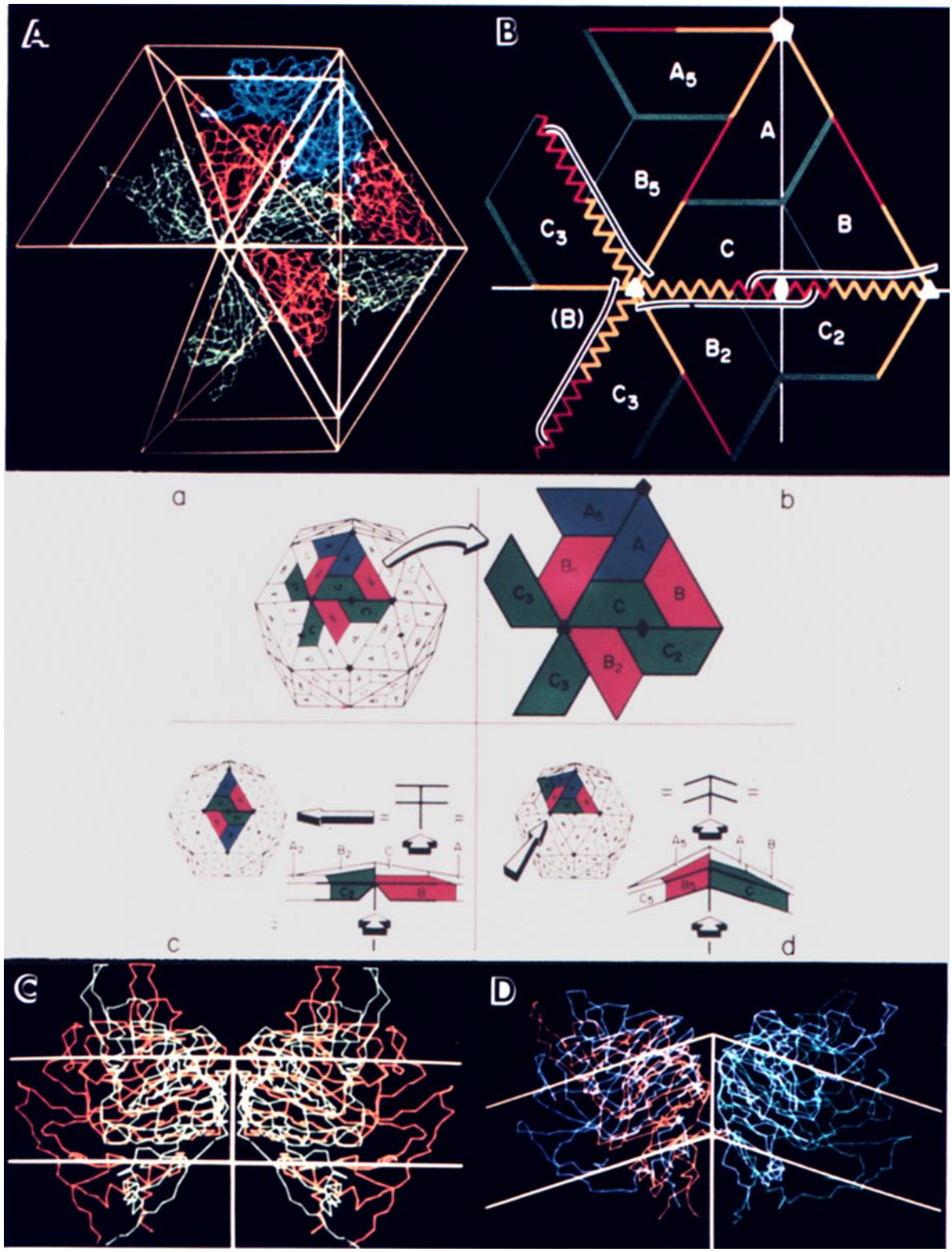

Fig. 4.

TABLE IV. Viral Capsids Containing ESAB-Fold*

Virus (family)	Triangulation no.	No. ESABs	Reference no.
Tomato bushy stunt	3†	180	22
Southern bean mosaic	3	180	21
Picornaviruses	1‡	180	18, 27
Cowpea mosaic	1**	180	28
Black beetle	3	180	This study

*An ESAB is an eight-stranded antiparallel beta barrel fold with the β-roll topology.
†Icosahedral asymmetric unit contains three identical subunits at the quasiequivalent A, B, and C positions illustrated in Figure 3b.
‡Icosahedral asymmetric units contains three nonidentical subunits (VP1, VP2, and VP3) each containing one ESAB at the A, C, and B positions, respectively.
**VP23 contains one ESAB (position A, Fig. 3b); VP37 contains two ESABs (positions B, C).

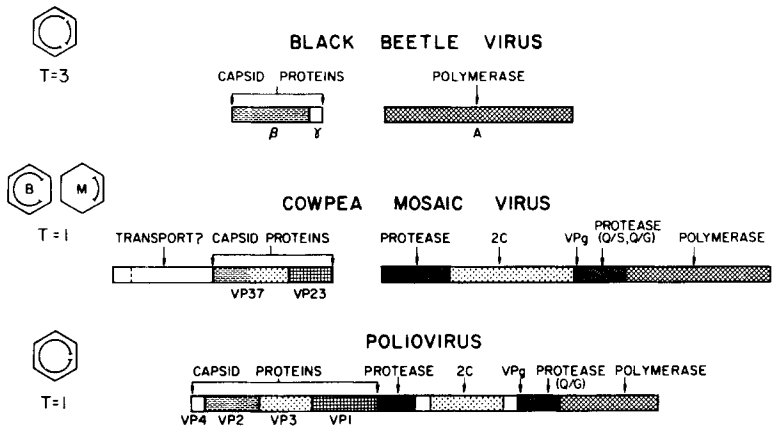

Fig. 5. Structure and genetic organization of a primitive insect virus (top), a plant virus with its genes coded on two polyproteins (middle), and an animal virus with all of its genes coded on a single polyprotein (bottom).

virus[26] the shells are all composed of 180 eight-stranded antiparallel β-barrels (ESAB) arranged with $T = 3$ symmetry (three identical chains in the asymmetric unit) or pseudo T-3 symmetry (3 nonidentical chains in the asymmetric unit). Thus, the shell structures of all these spherical viruses are preserved on both tertiary and quaternary levels. The coat proteins of cowpea mosaic virus and of the three picornaviruses (poliovirus, human rhinovirus 14, and Mengo), are positioned on a $T = 3$ lattice and are actually the result of fusion of the genes for three ESAB domains. This kind of gene fusion occurred not only in the coat protein but also in the vegative genes including polymerase, VPg, and several proteases (Fig. 5). Thus CpMV and picornaviruses probably evolved by modification and recombination of more primitive genes like those in black beetle virus. There is already convincing evidence of RNA recombination in both plant and animal viruses.[29]

What is the driving force for fusion of ESAB genes? One possibility is that three independent ESABs provide a mechanism for rapid evolution in the presence of neutralizing antibody. A mutation in the coat protein of a $T = 3$ virus introduces changes at three locations in the asymmetric structure unit; however, a similar mutation in a pseudo $T = 3$ capsid changes only one of the three ESAB positions. This permits pseudo $T = 3$ viruses to tolerate mutations that might otherwise be lethal in a $T = 3$ capsid and thereby allows greater potential for evolution. The pseudo $T = 3$ asymmetric unit in picornaviruses may therefore provide an important key to their success in coping with immune surveillance; the number of known picornavirus serotypes exceeds 200. In plants that possess no immune system, most spherical viruses have a $T = 3$ capsid. CpMV is an exception whose capsid and gene structure strongly resemble those of picornaviruses. It has already been suggested that a picorna-like ancestor of CpMV passed from animals to plants through a common insect vector.[30]

The simple genome structure and $T = 3$ capsid architecture both suggest that BBV represents a primitive stage in the evolution of a ribovirus. An example of how such a virus might have been created from cellular genes is illustrated in Figure 6. On the other hand the pyramid on the surface of its structure unit is unusually sophisticated (Fig. 3B,C) suggesting a significant evolutionary history. This pyramid may contribute to the extraordinary resistance of the virus to inactivation by heat, detergents, and other denaturants. Such stability may be important for survival in soil, the natural environment of its insect host. It is also a candidate for the receptor recognition site, since competition experiments indicate the presence of a BBV receptor site on the surface of *Drosophila* cells.

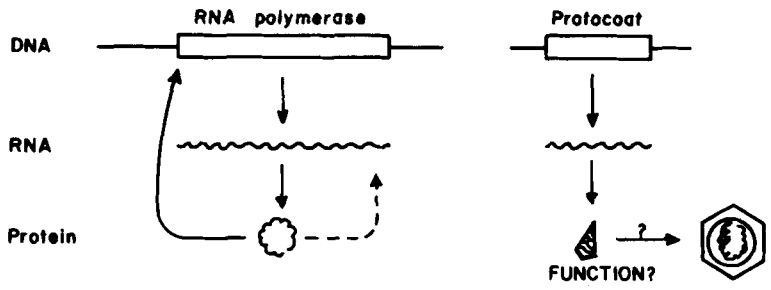

Fig. 6. Possible steps in evolution of a primitive plus-stranded ribovirus, such as BBV, from cellular "protocoat" and RNA polymerase genes. **Left**: a mutation in the cellular RNA polymerase gene allows the polymerase to recognize and replicate its own messenger RNA (RNA1) as template thus allowing it to multiply and mutate autonomously. **Right**: A hypothetical protocoat gene makes 180-subunit shells capable of recognizing and packaging its own mRNA (RNA2). Transfer of the recognition sequence in RNA2 into RNA1 enables both RNAs to be packaged in the protocoat shell and marks beginning of its evolution as a virus.

ACKNOWLEDGMENTS

This work was supported by Public Health Service grants GM34220 (to J.E.J. for the crystallographic analysis) and 9R37AI22813 (to R.R.R. for the biochemical analysis) from the National Institutes of Health. Protein sequencing was performed at the University of Wisconsin Biotechnology Center. T.M.G. was supported by PHS training grant T32G307215. Crystallographic computing on the Cyber 205 and on the graphics facility at Purdue University was supported by the National Science Foundation. The staff at LURE, Orsay, France and CHESS, Cornell University, Ithaca, New York are gratefully acknowledged for their assistance in crystallographic data collection. We thank Kathy Shuster and Sharon Fateley for their patience and help in the preparation of the manuscript.

Greg Kamer, Eddy Arnold, Gert Vriend, Michael Rossmann, Cynthia Stauffacher, and Ramakrishna Usha are gratefully acknowledged for many helpful discussions. M.V.H. and J.E.J. express their deep appreciation to Senator Richard Lugar and his staff for solving an immigration problem, thus permitting the early completion of this work.

REFERENCES

1. Longworth, J.F., Archibald, R.D. A virus of black beetle, Heteronychus arator (F.) (Coleoptera:Scarabaeidae). N.Z.J. Zool 2:233–236, 1975.
2. Friesen, P., Scotti, P., Longworth, J., Rueckert, R.R. Black beetle virus: Propagation in Drosophila line 1 cells and an infection-resistant subline carrying endogenous black beetle virus-related particles. J. Virol. 35:741–747, 1980.
3. Matthews, R.E.F. Classification and nomenclature of viruses. Intervirology 17:167–168, 1982.
4. Murphy, F.A., Scherer, W.F., Harrison, A.K., Dunne, W.G., Carey, G.W. Characterization of Nodamura virus, an anthropod transmissible picornavirus. Virology 40:1008–1021, 1970.
5. Johnson, J.E., Argos, P. Virus particle and stability—tricorna viruses. In: "The Viruses," Francki, R., Fraenkel-Conrat, H., Wagner, R. eds. New York: Plenum Press, 1985:19–56.
6. Dasmahaptra, B., Dasgupta, R., Ghosh, A., Kaesberg, P. Structure of the black beetle virus genome and its functional implications. J. Mol. Biol. 182:183–189, 1985.
7. Dasgupta, R., Ghosh, A., Dasmahaptera, B., Guarino, L., Kaesberg, P. Primary and secondary structure of black beetle virus RNA2, the genomic messenger for BBV coat protein precursor. Nucleic Acids Res. 12:7215–7223, 1984.
8. Longworth, J., Carey, G. A small RNA virus with a divided genome from Heteronychus arator (F.) (Coleoptera:scarabaeidae). J. Gen. Virol. 33:31–40, 1976.
9. Selling, B., Rueckert, R.R. Plaque assay for black beetle virus. J. Virol. 51:251–253, 1984.
10. Gallagher, T., Friesen, P.D., Rueckert, R.R. Autonomous replication and expression of RNA-1 from black beetle virus. J. Virol. 46:481–489, 1972.
11. Stoltzfus, C.M., Rueckert, R.R. Capside polypeptides of mouse elberfeld virus. J. Virol. 10:347–355, 1972.
12. Gilson, W., Gilson R., Rueckert, R.R. An automatic high-precision aerylamide gel fractionator. Anal. Biochem. 47:321–328, 1972.
13. Hosur, M.V., Schmidt, T., Tucker, R., Johnson, J.E., Selling, B.H., Rueckert, R.R. Black beetle virus-crystallization and particle symmetry. Virology 133:119–127, 1984.
14. Rossmann, M.G. Processing oscillation diffraction data for very large unit cells with an automatic convolution technique and profile fitting. J. Appl. Crystallogr. 12:225–238, 1979.
15. Rossmann, M.G., Leslie, A.G.W., Abdel-Meguid, S.S., Tsukihara, T. Processing and post-refinement of oscillation camera data. J. Appl. Crystallogr. 12:570–581, 1979.
16. Argos, P., Rossmann, M.G.: A method to determine heavy-atom positions for virus structures. Acta Cryst. B32:2975–2979, 1976.
17. Johnson, J.E. Appendix II: Averaging of electron density maps. Acta Crystallogr. B34:576–577, 1978.
18. Rossmann, M.G., Arnold, E., Erickson, J.W., Frankenberger, E.A., Griffith, J.P., Hecht, H.J., Johnson, J.E., Kamer, G., Luo, M., Mosser, A.G., Rueckert, R.R., Sherry, B., Vriend, G. Structure of a human common cold virus and functional relationship to other picornaviruses. Nature 317:145–153, 1985.
19. Caspar, D.L.D., Klug, A. Physical principles in the construction of regular viruses. Cold Spring Harbor Symp. Quant. Biol. 27:1–24, 1962.
20. Jones, T.A. Frodo A graphics fitting program for macromolecules. In: "Computational Crystallography." Sayre D., ed. New York: Oxford University Press, 1982:303–317.
21. Abad-Zapatero, C., Abdel-Meguid, S.S., Johnson, J.E., Leslie, A.G.W., Rayment, I., Rossmann, M.G., Suck, D., Tsukihara, T. Structure of southern bean mosaic virus at 2.8 Å resolution. Nature 286:33–39, 1980.
22. Harrison, S., Olson, A.J., Schutt, C.E., Winkler, F.K., Bricogne, G. Tomato bushy stunt virus at 2.9 Å resolution. Nature 276:368–373, 1978.
23. Erickson, J., Rossmann, M.G. Assembly and crystallization of a $T = 1$ icosahedral particle from trypsinized southern bean mosaic virus coat protein. Virology 116:128–136, 1982.
24. Tremaine, J., Ronald, W.P., Agrawal, H.O. Same tryptic peptides of bromovirus proteins. Virology 83:404–412, 1977.
25. Rossmann, M.G., Argos, P.: Protein folding. Annu. Rev. Biochem. 50:497–532, 1981.

26. Liljas, L., Unge, T., Jones, T.A., Fridborg, K., Lovgren, S., Skoglund, U., Strandberg, B. Structure of satellite tobacco necrosis virus at 3.0 Å resolution. J. Mol. Biol. 159:93–108, 1982.
27. Hogle, J., Chow, M., Filman, J. Three-dimensional structure of poliovirus at 2.9 Å resolution. Science 229:1358–1365, 1985.
28. Stauffacher, C., Usha, R., Harrington, M., Schmidt, T., Hosur, M.V., Johnson, J.E.: The Structure of Cowpea Mosaic Virus at 3.5 Å Resolution. In "Crystallography in Molecular Biology." Moras, D., Suck, D., B. Strandberg, B.O., Dreuth, J., Blundel T, eds. New York: Plenum Publishing Corporation 308, 1987:293–308.
29. Kaesberg, P. Evolution and genome structure, In: "Plus-Strand Viruses." Brinton M, Rueckert R, eds. Los Angeles: UCLA, 1987:3–7.
30. Goldbach, R.W. Molecular evolution of plant RNA viruses. Annu Rev Phytopathology 24:289, 1986.